ACS APPLIED MATERIALS & INTERFACES

LETTER

www.acsami.org

Multiphase Adhesive Coacervates Inspired by the Sandcastle Worm

Sarbjit Kaur, G. Mahika Weerasekare, and Russell J. Stewart*

Department of Bioengineering, University of Utah, Salt Lake City, Utah 84112, United States

Supporting Information

ABSTRACT: Water-borne, underwater adhesives were created by complex coacervation of synthetic copolyelectrolytes that mimic the proteins of the natural underwater adhesive of the sandcastle worm. To increase bond strengths, we created a second polymer network within cross-linked coacervate network by entrapping polyethylene glycol diacrylate (PEG-dA) monomers in the coacervate phase. Simultaneous polymerization of PEG-dA and cross-linking of the coacervate network resulted in maximum shear bond strengths of ~1.2 MPa. Approximately 40% of the entrapped PEG-dA polymerized based on attenuated total reflectance-Fourier transform infrared spectroscopy. The monomer-filled coacervate had complex flow behavior, thickening at low shear rates and then thinning suddenly with a 16-fold drop in viscosity at shear rates near 6 s^{-1}. The microscale structure of the complex coacervates resembled a three-dimensional porous network of interconnected tubules. The sharp shear thinning behavior is conceptualized as a structural reorganization between the interspersed phases of the complex coacervate. The bond strength and complex fluid behavior of the monomer-filled coacervates have important implications for medical applications of the adhesives.

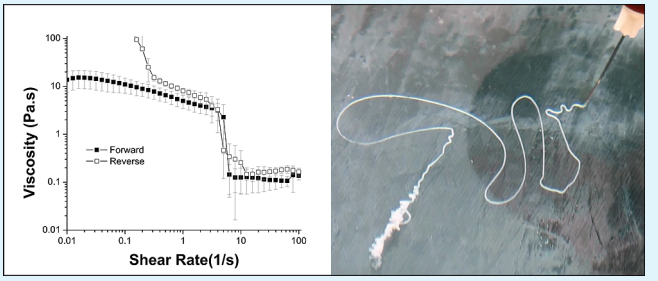

KEYWORDS: complex coacervates, multiphase coacervates, underwater adhesives, polymer networks, biomimetic, biomaterials, bioadhesives

Adhesive bonding in watery environments with common synthetic adhesives is confounded, in general, by poor interfacial adhesion leading to eventual failure by infiltration of water into the joint. Aquatic environments are populated with diverse organisms that have evolved a multitude of workable solutions to the underwater adhesion problem. Natural underwater adhesives have therefore been studied as potential sources of materials or concepts with the goal of creating or improving synthetic adhesives for wet applications, including repair of living tissues. One such model is the underwater adhesive of the Sandcastle worm (*Phragmatopoma californica*), a marine polychaete.[1−3] The Sandcastle worm employs an ingenious strategy to construct composite mineralized shells; the mineral phase is gathered from its environment preformed as sandgrains and shell fragments that are then glued together with small dabs of an underwater adhesive.[1]

The sandcastle worm glue is comprised of oppositely charged proteins and divalent cations.[2,3] Copolyelectrolytes with the same chemical side chains (phosphates and amines) and in the same proportions as the natural proteins were synthesized. When mixed under the right conditions, the synthetic copolyelectrolytes condensed into fluid complex coacervates.[4,5] As the basis for underwater adhesives, complex coacervates have several ideal properties: the dense, phase-separated fluids sink in water, are sufficiently cohesive that they do not mix with water on a time scale of several minutes, and readily adhere to wet surfaces, all of which allows the adhesive to stay in place where it is applied underwater. The adhesive becomes load-bearing by triggered solidification of the complex coacervate after application. The sandcastle worm glue sets within 30 s through pH-triggered solidification of a polyphosphorylated protein and Ca^{2+} and Mg^{2+}.[2,6] The initial set is followed up over several hours by covalent cross-linking through 3,4-dihydroxy-L-phenylalanine (dopa) residues. Both the pH-triggered set and dopa-mediated cross-linking were replicated in biomimetic adhesive coacervates.[4,5]

Though the natural sandcastle glue is suitable for the dimensions and lifecycle of sandcastle worms, it is not particularly strong, around 300 kPa.[7] Biomimetic adhesives will have to be much stronger than the natural adhesive to find broad utility. Incorporation of micro- or nanophases into the bulk adhesive phase is a well-known strategy for increasing adhesive bond strengths.[8] Our strategy for incorporation of an additional phase into our biomimetic adhesive was to form the coacervate in the presence of a water-soluble neutral monomer, as a first example, polyethylene glycol-diacrylate (PEG-dA). Polymerizable monomers dissolved in the aqueous copolyelectrolyte solutions become incorporated into the dense coacervate phase, which is mostly water by weight. Polymerization created a second polymer network within the coacervated copolyelectrolyte network. The coacervate functioned, in effect, as a container for the polymerizable monomers that can be accurately delivered

Received: January 21, 2011
Accepted: March 9, 2011
Published: March 16, 2011

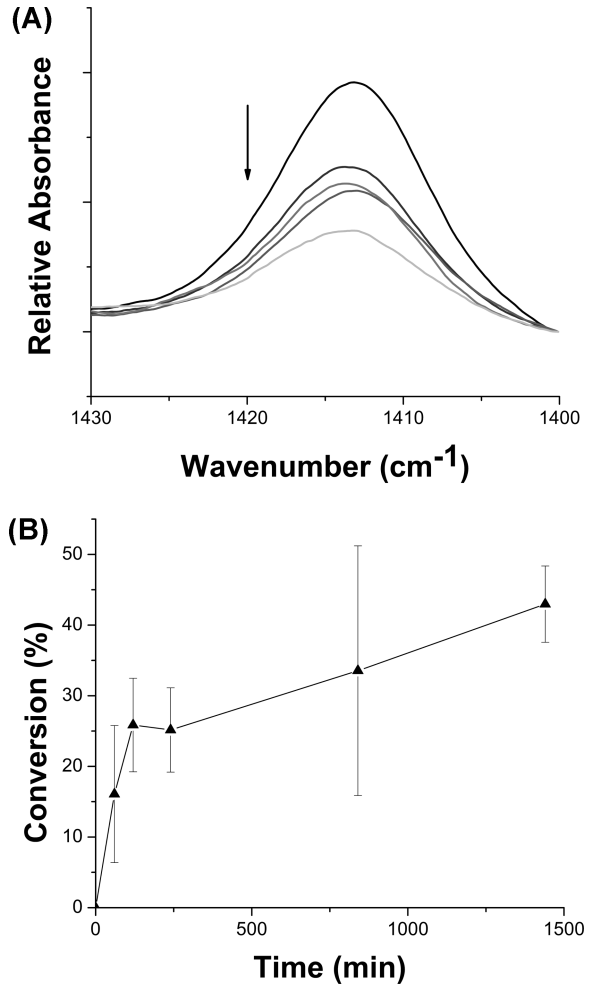

Figure 1. ATR-FTIR Study of 11.4 wt % PEG-dA complex coacervate. (A) Spectrum of acrylate group at 1415 cm^{-1} (↓ indicating peak decreasing over time after polymerization). (B) Time course of PEG-dA conversion over 24 h. Error bars: ± s.d. (n = 3).

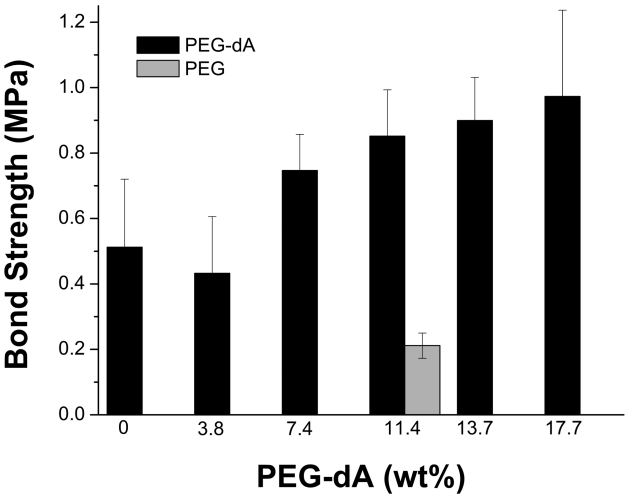

Figure 2. Shear bond strength of PEG-dA filled complex coacervates. The coacervate network was oxidatively cross-linked and PEG-dA polymerized by the simultaneous addition of $NaIO_4$ and APS/TEMED, respectively. Bonds were cured under water for 24 h at 25 °C. Gray column: coacervate filled with 15 wt % nonacrylated PEG and cured with $NaIO_4$ and APS/TEMED. Error bars: ± s.d. (n = 5).

underwater before polymerization of the second internal polymer network is initiated.

Coacervates were formed with 2-(methacryloyloxy) ethyl phosphate dopamine methacrylamide (poly(MOEP-co-DMA)), poly(acrylamide-co-aminopropyl methacrylamide) and Ca^{2+}, as described in detail previously,[4] in solutions containing nominal wt % concentrations of 0, 5, 10, 15, 20, and 25 PEG-dA (MW 700 g/mol). Dense complex coacervates phase separated from the solutions. The concentration of PEG-dA entrapped in the coacervate phase was determined by Attenuated Total Reflectance-Fourier Transform Infrared Microscopy (ATR-FTIR). The absorbance peak at 1415 cm^{-1} was compared to the 1415 cm^{-1} acrylate groups of standard solutions of PEG-dA in water (Figure 1A).[9,10] On average the PEG-dA concentration in the coacervate was 73% of the initial concentration in solution. Above 25 wt % PEG-dA the coacervates were too viscous to work with conveniently. Free radical polymerization of entrapped PEG-dA was initiated by adding ammonium persulfate (APS) and tetramethylethylenediamine (TEMED) to the complex coacervate. The extent of PEG-dA polymerization within the coacervate was determined from the 1415 cm^{-1} ATR-FTIR peak corresponding to the acrylate functional group (Figure 1B). The complex coacervate containing 11.4 wt % PEG-dA reached ~40% conversion after 24 h.

The shear bond strengths of the PEG-dA filled adhesive coacervates were determined in lap shear tests with polished aluminum adherends. Cross-linking of the coacervate network through the *o*-dihydroxyphenyl side chains of poly(MOEP-co-DMA) and the amine side chains of poly(acrylamide-co-aminopropyl methacrylamide) was initiated by addition of $NaIO_4$. Free radical polymerization of PEG-dA was initiated simultaneously by addition of APS and TEMED. Immediately after initiation the coacervates were applied to wet Al adherends. The bonds were cured for 24 h fully submerged in water (22 °C) before loading to failure on a material testing system. The maximum bond strengths increased with increasing PEG-dA (Figure 2), nearly doubling from a mean of 512 ± 208 kPa without PEG-dA to a mean of 973 ± 263 kPa with 17.7 wt % PEG-dA. Maximum loads were ~1.2 MPa, more than four times higher than estimated bond strengths of the natural sandcastle glue[7] and mussel adhesive plaque byssal thread assemblies.[11] The shear modulus, approximately 25 MPa, was not statistically different between any of the PEG-dA concentrations. To confirm the increased bond strength was due to polymerization of PEG-dA, we formed coacervates with 15 wt % nonacrylated PEG (MW 400 g/mol) and treated with $NaIO_4$ and APS/TEMED. The underwater bond strengths were 211 ± 39 kPa, less than 25% of the PEG/coacervate bond strengths.

The flow behavior is of critical importance for adhesives based on complex fluids such as coacervates. For medical applications, the viscosity should be sufficiently high at low shear rates that the adhesive does not flow away from the application site, and yet low enough at high shear rates that it can be conveniently applied through a narrow gauge cannula, or catheter, without high pressure. At the same time, it is imperative to recognize shear-induced, irreversible structural transitions at high shear rates that may compromise cohesive bond formation. The viscosities of the adhesive complex coacervates containing 0 and 11.4 wt % PEG-dA were investigated as a function of shear rate using a cone and

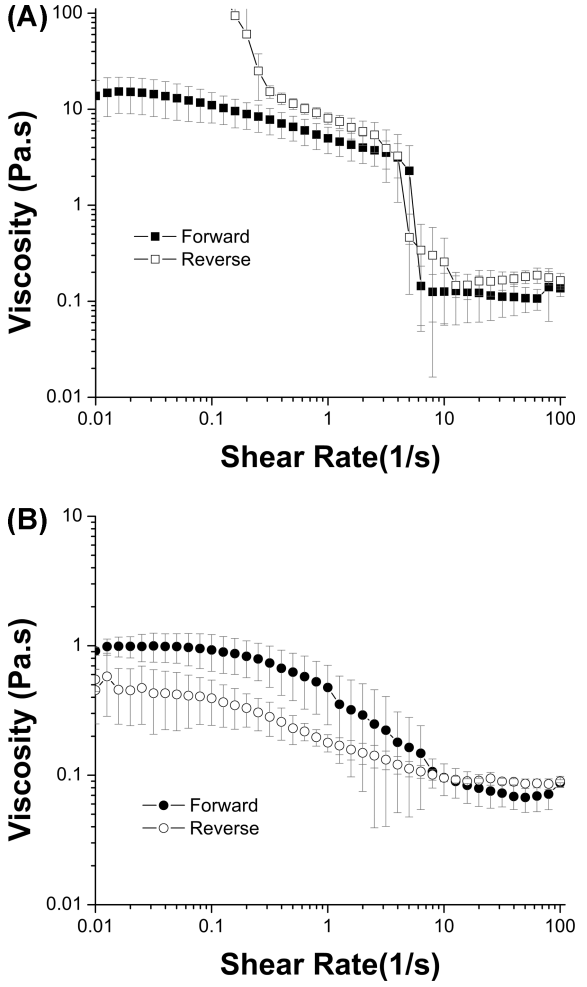

Figure 3. Flow curves of complex coacervates under steady shear. (A) Filled coacervates of 11.4 wt % PEG-dA: low to high shear rate (closed square) and high to low shear rate (open square). (B) Unfilled coacervate: low to high shear rate (closed circle), and reverse (open circle). Symbols and error bars are the average viscosity and s.d. at each shear rate of three independent coacervate samples.

plate geometry (Figure 3). At low shear rates (0.01 s^{-1}) the viscosity of the 11.4 wt % PEG-dA filled coacervate (13.8 ± 6.2 Pa s) was substantially higher than the complex coacervate with 0 wt % PEG-dA (0.9±0.1 Pa s). With increasing shear rate the PEG-dA filled coacervates first thickened, then steadily thinned until a sudden 16-fold drop in viscosity occurred at a shear rate of 6 s^{-1} (Figure 3A). The shear thinning behavior was reversible; viscosity recovered with little hysteresis as the shear rate was decreased. The complex coacervate without PEG-dA shear thinned as well but did not display a similar sudden sharp drop in viscosity (Figure 3B).

The flow curves of the complex coacervate containing PEG-dA monomers are similar to other coacervate systems that have been investigated rheologically. Whey protein and gum arabic coacervates displayed a similarly abrupt shear thinning transition that was accompanied by an increase in turbidity.[12] The transition was reversible. Polycation/mixed micelle coacervates, above a certain temperature, underwent a dramatic shear rate-dependent drop in viscosity before visibly phase separating.[13] In both cases, the visible changes suggested the abrupt shear thinning

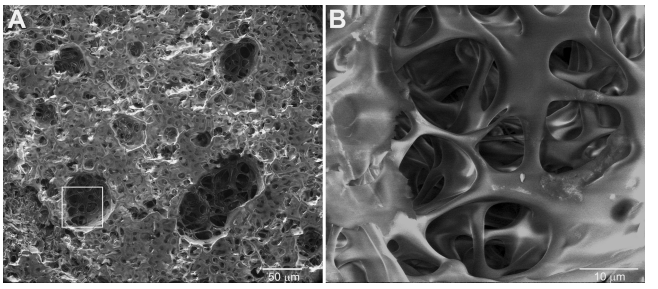

Figure 4. SEM Images of fractured surfaces of lyophilized complex coacervates. (A) 700×, (B) 5000×.

events were due to microscale structural reorganizations of the interspersed phases of the complex coacervates. The quiescent nanoscale molecular structure of the complex coacervates were conceptualized as beads on compacted strings; globular whey proteins on gum arabic molecules in the first case, polyanionic mixed micelle beads on polyamine strings in the second case.[14] Abrupt shear thinning was attributed to shear-induced elongation of the beaded string structures, resulting in increased lateral intercomplex associations, and coalescence of nanocomplexes into dense microphases.

The rich and complex flow behavior of the PEG-dA filled coacervates suggested that similar shear-induced, reversible structural reorganization may occur within the PEG-dA filled coacervates. Unsheared complex coacervates with and without PEG-dA were frozen, lyophilized, and examined by scanning electron microscopy (SEM). The coacervates had a porous three-dimensional network of tubular structures (Figure 4) reminiscent of the sponge-like network of tubules observed in other complex coacervates by cryo-TEM.[15] There were no structural differences apparent between coacervates with and without PEG-dA monomers. Based on the flow behavior and SEM micrographs, a conceptual diagram of the PEG-dA filled complex coacervate before and after the shear-induced structural transition is shown in Figure 5. The quiescent coacervate is pictured as a dense, interconnected, colloid-rich network interspersed within a watery, colloid-depleted network containing PEG-dA (Figure 5A). Above a critical shear rate, the interspersed networks may undergo shear-banding (Figure 5B), a phenomenon in which the components of a complex fluid phase separate into distinct bands under shear.[16−18]

The practical significance of the shear thinning of the PEG-dA filled coacervates is demonstrated in the video in the Supporting Information. A 11.4 wt % PEG-dA filled coacervate was loaded into a 1 mL syringe fitted with a 27 gauge cannula. Despite the relatively high initial viscosity, it took little manual effort to eject a fine cohesive thread of the PEG-dA filled coacervate under water. The shear rate during ejection was estimated to be 750 s^{-1}. The water-borne threads were denser than water, maintained their shape, and adhered where they contacted the glass surface. The coacervate also adhered when applied underwater to vertical glass surfaces. In principle, the coacervated threads, or any pattern of threads, can be cross-linked in place by coinjection of polymerization initiators. The ability to accurately deliver adhesive through a fine cannula or catheter will allow precise and less invasive repair of bone fractures[19] and other tissues.

In summary, the bond strength of the biomimetic adhesive coacervates was substantially improved, to well above the estimated bond strengths of natural bioadhesives, by incorporating a

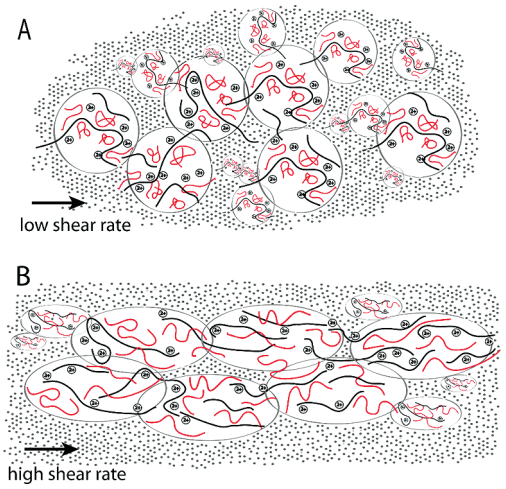

Figure 5. Conceptual diagram of the structure of the PEG-dA filled complex coacervate. (A) In the quiescent state, the electrostatically associated nanocomplexes form a fluid, interconnected, three-dimensional network. An aqueous phase containing PEG-dA is interspersed within the pores of the connected network of nanocomplexes. (B) At a critical shear rate, the nanocomplexes may be elongated leading to additional lateral interactions and a second, reversible macrophase separation.

second polymer network into the coacervate network. The viscous PEG-dA filled coacervate could be easily ejected through a fine gauge cannula as a result of reversible shear-thinning. The threads maintained their form underwater and adhered to wet glass surfaces. The successful incorporation of high concentrations of water-soluble monomers demonstrated that, in principle, almost any water-soluble molecules can be contained in a complex coacervate and precisely delivered in a wet environment, including noninvasive delivery into the body. Such properties merit further evaluation of the filled adhesive coacervates as injectable drug delivery depots in addition to their potential as wet field medical adhesives. Work in progress is focused on incorporating more and different types of nano- and microphases into complex coacervates to further improve underwater bond strengths.

■ ASSOCIATED CONTENT

Supporting Information. Experimental procedures and additional figures (PDF) and supplemental video (QuickTime). This material is available free of charge via the Internet at http://pubs.acs.org.

■ AUTHOR INFORMATION

Corresponding Author

*E-mail: rstewart@eng.utah.edu. Phone: 801-581-8581.

■ ACKNOWLEDGMENT

Support from the NIH (EB006463) and the Office of Naval Research (N00014-10-1-0108) are gratefully acknowledged. We thank Daniel Taggart for SEM.

■ REFERENCES

(1) Jensen, R. A.; Morse, D. E. *J. Comp. Physiol. B.* **1988**, *158*, 317–324.
(2) Stewart, R. J.; Weaver, J. C.; Morse, D. E.; Waite, J. H. *J. Exp. Biol.* **2004**, *207*, 4727–4734.
(3) Zhao, H.; Sun, C.; Stewart, R. J.; Waite, J. H. *J. Biol. Chem.* **2005**, *280*, 42938–42944.
(4) Shao, H.; Bachus, K. N.; Stewart, R. J. *Macromol. Biosci.* **2009**, *9*, 464–471.
(5) Shao, H.; Stewart, R. J. *Adv. Mater.* **2010**, *22*, 729–733.
(6) Stevens, M. J.; Steren, R. E.; Hlady, V.; Stewart, R. J. *Langmuir* **2007**, *23*, 5045–5049.
(7) Sun, C.; Fantner, G. E.; Adams, J.; Hansma, P. K.; Waite, J. H. *J. Exp. Biol.* **2007**, *210*, 1481–1488.
(8) Kinloch, A. J.; Lee, J. H.; Taylor, A. C.; Sprenger, S.; Eger, C.; Egan, D. *The Journal of Adhesion* **2003**, *79*, 867–873.
(9) Witte, R. P.; Blake, A. J.; Palmer, C.; Kao, W. J. *J. Biomed. Mater. Res., A.* **2004**, *7*, 508–518.
(10) Kang, G.; Cao, Y.; Zhao, H.; Yuan, Q. *J. Membr. Sci.* **2008**, *318*, 227–232.
(11) Burkett, J. R.; Wojtas, J. L.; Cloud, J. L.; Wilker, J. J. *J. Adhes.* **2009**, *85*, 601–615.
(12) Weinbreck, F.; Wientjes, R. H. W.; Nieuwenhuijse, H.; Robijn, G. W.; Kruif, C. G. *J. Rheol.* **2004**, *48*, 1215–1228.
(13) Dubin, P. L.; Li, Y.; Jaeger, W. *Langmuir* **2008**, *24*, 4544–4549.
(14) Liberatore, M. W.; Wyatt, N. B.; Henry, M.; Dubin, P. L.; Foun, E. *Langmuir* **2009**, *25*, 13376–13383.
(15) Hwang, D. S.; Zeng, H.; Srivastava, A.; Krogstad, D. V.; Tirrell, M.; Israelachvili, J. N.; Waite, J. H. *Soft Matter* **2010**, *6*, 3232–3236.
(16) Makhloufi, R.; Decruppe, J. P.; Ait-Ali, A.; Cressely, R. *Europhys. Lett.* **1995**, *32*, 253–258.
(17) Butler, P. *Curr. Opin. Colloid Interface Sci.* **1999**, *4*, 214–221.
(18) Barnes, H. A.; Hutton, J. F.; Walters, K. *An Introduction to Rheology*; Elsevier: Amsterdam, 1989.
(19) Winslow, B. D.; Shao, H.; Stewart, R. J.; Tresco, P. A. *Biomaterials* **2010**, *31*, 9373–9381.